JOURNAL OF VIROLOGY, Apr. 1982, p. 153–164
0022-538X/82/040153-12$02.00/0

Vol. 42, No. 1

RNA-Dependent RNA Polymerase Activity in Coronavirus-Infected Cells

DOUGLAS E. DENNIS AND DAVID A. BRIAN*

Department of Microbiology, The University of Tennessee, Knoxville, Tennessee 37916

Received 26 October 1981/Accepted 15 December 1981

An enzymatic activity which incorporates [^{3}H]UMP into acid-precipitable material in the presence of endogenous template was found in the cytoplasm of porcine cells infected with the transmissible gastroenteritis virus of swine. This activity was not found in uninfected control cells, nor was it found in purified virus. The activity was associated with the mitochondrial fraction of infected cells, suggesting that the enzyme is membrane bound. The activity required the presence of all three ribonucleoside triphosphates in addition to [^{3}H]UTP, and it was not inhibited by actinomycin D. The heated product was digested by RNase but not by DNase. Mg^{2+} was required for enzymatic activity, and its optimal concentration was approximately 5 mM. The size of the in vitro products was compared by electrophoresis with that of in vivo-synthesized virus-specified RNA to confirm the viral specificity of the polymerase activity. Virus-specified RNA from infected cells consisted of 10 species of single-stranded, polyadenylated RNA with molecular weights of 6.8×10^6, 6.2×10^6, 3.15×10^6, 1.40×10^6, 1.05×10^6, 0.94×10^6, 0.66×10^6, 0.39×10^6, 0.34×10^6, and 0.24×10^6. In vitro-synthesized RNA consisted of a high-molecular-weight species, of apparently higher molecular weight than genomic RNA, and two single-stranded species that electrophoretically comigrated with the species of 1.40×10^6 and 0.66×10^6 molecular weight made in vivo.

Coronaviruses were originally classified as a separate family primarily on the basis of ultrastructural characteristics (37). Recent information regarding the replicational strategy of representative coronaviruses confirms the uniqueness of this family. First, it has been shown for avian infectious bronchitis virus (19, 20, 30), mouse hepatitis virus (16, 38, 39), and porcine transmissible gastroenteritis virus (TGEV) (4) that the RNA genome is single stranded, nonsegmented, polyadenylated, and infectious. The genome is therefore of positive polarity (3). This property is shared by animal viruses only in the picornavirus and togavirus families, families that are clearly ultrastructurally distinct from coronaviruses (27, 36). Second, for both avian infections bronchitis virus (34, 35) and mouse hepatitis virus (32), multiple (five in the case of the avian virus and six in the case of the mouse virus) subgenomic, polyadenylated, intracytoplasmic RNA species are synthesized during virus replication. Each of these presumably functions as mRNA, but in vitro translation studies to date have confirmed that only some are functional mRNA species (29, 31). This pattern of transcription is not shared by picornaviruses and togaviruses.

Our objective was to further characterize coronavirus replication and to compare it with the replication of other positive strand viruses. By analogy with the picornaviruses and togaviruses, one would not expect to find an RNA-dependent RNA polymerase as part of the coronavirion, but would expect to find such an enzyme in coronavirus-infected cells. In this paper we report that we were unable to detect an RNA-dependent RNA polymerase in purified virions, but did find it associated with apparent membrane structures in infected cells. The polymerase synthesized two RNA species in vitro that electrophoretically comigrated with 2 of the 10 single-stranded, polyadenylated species made in vivo. A high-molecular-weight species, of apparently higher molecular weight than genomic RNA, was also synthesized during the in vitro reaction.

MATERIALS AND METHODS

Cells. The epithelioid swine testicle cell line ST, developed by McClurkin (23), was grown as previously described (4) except that the growth medium contained 5% fetal calf serum (GIBCO Laboratories, Grand Island, N.Y.) and 5% calf serum (Kansas City Biologicals, Inc., Lanexa, Kans.). The human embryonic lung cell line MRC-5 was obtained from Flow Laboratories, Inc., Rockville, Md., and was propagated as described for ST cells.

Viruses. Clone 116 of the Purdue strain of swine TGEV was obtained from E. Bohl, Ohio Agricultural

Research and Development Center, Wooster, Ohio. The virus was cloned twice again by us. Cloned virus was passaged twice at a multiplicity of <0.1 PFU per cell, and then viral stocks were prepared from passages 3 through 6 by infecting cells at a multiplicity of approximately 10 PFU per cell. Viral titers ranging from 10^8 to 10^9 PFU per ml were obtained in stock virus preparations. The Indiana strain of vesicular stomatitis virus was obtained from A. Brown, University of Tennessee, Knoxville. Poliovirus, type I (attenuated), was obtained from the American Type Culture Collection, Rockville, Md.

Infection of cells, virus purification, and virus titration. For TGEV and vesicular stomatitis virus the methods used for the infection of cells, virus purification, and virus titration have been described (4). The same method was used for growing poliovirus except that MRC-5 cells were used. Poliovirus was grown for 24 h in the presence of [^{3}H]uridine, 40 μCi/ml, and virus in clarified supernatant fluids was used as a sedimentation coefficient marker.

RNA polymerase assay. The assay for virion-associated RNA-dependent RNA polymerase was essentially that described by Huang et al. for the Newcastle disease virus-associated enzyme (14). In a standard reaction, 50 μl of purified virus, suspended to a concentration of 0.2 to 0.5 mg/ml in reticulocyte standard buffer (10 mM Tris hydrochloride [pH 7.4]–100 mM NaCl–1.5 mM $MgCl_2$), was assayed in a 300-μl solution (total volume) containing 50 mM Tris-hydrochloride (pH 7.3), 5.3 mM magnesium acetate, 0.1 M sodium chloride, 3.3 mM 2-mercaptoethanol, 830 μg of Triton N-101 per ml, 0.83 μM [5-^{3}H]UTP (44 cpm/fmol) or 2.20 μM [8-^{3}H]GTP (16.7 cpm/fmol), and 0.67 mM each of ATP, CTP, and GTP (or UTP when [^{3}H]GTP was used). The amount of labeled substrate incorporated into product in 30 min at 33°C was measured by collecting the product on membrane filters (0.45 μm; Amicon Corp.) after precipitation with 5% trichloroacetic acid–0.05 M sodium pyrophosphate at 0°C. Dried filters were counted in toluene containing 4 mg of 2,5-bis-(5′-*tert*-butyl-benzoxazolyl-[2′]) thiophene per ml.

The assay for cell-associated, RNA-dependent RNA polymerase was a modification of that described by Arlinghaus and Polatnick (2) for the foot-and-mouth disease virus enzyme. In a standard reaction, 50 μl of sample, suspended to a protein concentration of 10 to 20 mg/ml in 0.25 M sucrose–1.5 mM $MgCl_2$–40 μg of dextran sulfate per ml–0.28% (wt/wt) deoxycholate, was assayed in a 200-μl solution (total volume) containing: 50 mM Tris-hydrochloride (pH 8.0), 5 mM magnesium acetate, 10 mM phosphoenolpyruvic acid, 40 μg of pyruvate kinase per ml, 17.5 mM 2-mercaptoethanol, 20 μg of actinomycin D per ml, 40 μg of dextran sulfate per ml, 1.25 μM [5-^{3}H]UTP (44 cpm/fmol) or 3.30 μM [8-^{3}H]GTP (16.7 cpm/fmol), and 0.5 mM each of ATP, CTP, and GTP (or UTP when [^{3}H]GTP was used). To detect enzyme activity, the amount of labeled substrate incorporated into product in 60 min at 37°C was measured by collecting the product on membrane filters as described above. In examinations of the products of the enzyme reaction, only 5-^{3}H-radiolabeled substrates were used, and reaction times were held to 15 min or less to minimize the likelihood of RNase degradation of the reaction products. RNA was then extracted as described below.

Subcellular fractionation. Batches of 2×10^8 to 8×10^8 cells (representing one to four confluent roller bottle cultures) were treated as described in the various experimental protocols with regard to infection and radioisotopic labeling. At the designated times, cells were drained and washed five times with ice-cold TN buffer (10 mM Tris-hydrochloride [pH 7.4]–0.1 M NaCl). All further steps were done at 0 to 4°C. Cells were scraped into TN buffer and pelleted by centrifugation at 500 × *g* for 10 min. Cells were then suspended in 10 ml of a 0.3 M sucrose solution, allowed to swell for 10 min, and disrupted by use of 15 strokes in a tight-fitting glass Dounce homogenizer. Cellular disruption and nuclear breakage were monitored by light microscopy. Less than 2% of the cells remained intact after this treatment. The suspension was centrifuged at 650 × *g* for 7 min, and the pellet, which contained nuclei and other large debris, was designated the nuclear fraction. The resultant supernatant was centrifuged at 13,000 × *g* for 20 min in a Beckman JA-20 rotor, and the pellet formed was designated the mitochondrial fraction. The resultant supernatant was designated the postmitochondrial fraction and was either analyzed directly for measurement of trichloroacetic acid-precipitable radioactive material or was further treated with 10% polyethylene glycol to form a precipitate which was then resuspended and analyzed for enzymatic activity.

For analysis of the products of the in vitro reaction, a postnuclear pellet was prepared and was used as the source of the enzyme and endogenous template. Nuclei and large debris were pelleted at 650 × *g* for 7 min, and the supernatant was layered onto 20 ml of 10 mM Tris-hydrochloride–40 μg of dextran sulfate 500 (Sigma Chemical Co.) per ml–20% (wt/wt) sucrose in a 38-ml centrifuge tube. The pellet formed by centrifugation at 60,000 × *g* for 1.5 h in a Sorvall AH-627 rotor was drained, suspended in a solution of 0.25 M sucrose–1.5 mM $MgCl_2$–40 μg of dextran sulfate 500 (Sigma Chemical Co.) per ml–2.8 mg of sodium deoxycholate per ml to a final protein concentration of 10 to 20 mg/ml, and used immediately or divided into small portions and stored at −80°C. Samples retained approximately 75% of their polymerase activity after storage for 1 month.

RNA extraction. For extraction of RNA from the postnuclear pellet, the postnuclear pellet from 2×10^8 to 8×10^8 cells was dissolved in 2 ml of TNE (10 mM Tris-hydrochloride [pH 7.5]–0.1 M NaCl–1 mM EDTA)–2% sodium dodecyl sulfate and 0.1 mg of proteinase K, incubated at 37°C for 15 min, and phenol extracted once with an equal volume of TNE-saturated phenol. RNA was precipitated at −20°C with 2 volumes of 95% ethanol.

For analysis of the in vitro polymerase reaction products, the reaction was terminated after 15 min by the addition of 0.25 volume of 5× TNE–10% sodium dodecyl sulfate and 0.1 mg of crystalline proteinase K. The mixture was incubated at 37°C for 15 min and then phenol extracted once with an equal volume of TNE-saturated phenol. The RNA was precipitated at −20°C with 2 volumes of 95% ethanol for at least 5 h. The precipitate was dissolved in 0.5 ml of 10 mM Tris-hydrochloride (pH 7.5) and reprecipitated after the addition of 55 μl of 2 M sodium acetate. This step was repeated twice. All solutions were treated with 0.1% diethylpyrocarbonate for 24 h prior to use.

Preparation of cellular and viral marker RNA spe-

cies. [^{3}H]uridine-labeled cellular and viral RNA marker species were prepared as previously described (4).

Agarose gel electrophoresis and fluorography. The method of Lehrach et al. was used to analyze RNA by electrophoresis in agarose gels (18). Briefly, RNA samples were heated in 2.2 M formaldehyde–50% (wt/wt) formamide–18 mM Na_2HPO_4–2 mM NaH_2PO_4 for 5 min at 60°C immediately prior to electrophoresis. Electrophoresis buffer was 2.2 M formaldehyde–1.8 mM Na_2HPO_4–2 mM NaH_2PO_4. Slab gels of 0.75% agarose were used with a horizontal apparatus that had dimensions of 11 by 13 cm. Gels were 6 mm thick. Electrophoresis was carried out with the use of 50 V of constant voltage with a current of approximately 50 mA. Upon termination of electrophoresis, gels were dehydrated in two sequential baths of 10 volumes of methanol for 2.5 h each. Methanol was then blotted from the gels with filter paper until the gels were approximately 1.5 mm thick, at which time they were treated with Enhance (New England Nuclear Corp., Boston, Mass.) and dried in a slab gel drier (Hoefer Scientific Instruments, Inc.) under vacuum and low heat. Gels were fluorographed by the method of Laskey and Mills (17).

Oligodeoxythymidylate-cellulose chromatography. RNA extracted from 2×10^8 infected cells was dissolved in high-salt buffer (10 mM Tris [pH 7.5]–0.12 M NaCl–1 mM EDTA–0.2% SDS) and was bound to 500 mg of oligodeoxythymidylate-cellulose, type 77F (P-L Biochemicals, Inc.), that had been equilibrated with high-salt buffer. RNA eluting with low-salt buffer (10 mM Tris [pH 7.5]–1 mM EDTA–0.2% sodium dodecyl sulfate) was considered to be polyadenylated RNA.

Materials. [^{3}H]uridine (8 Ci/mmol) was obtained from Schwartz/Mann. $^{32}P_i$ (144 Ci/mg) was obtained from Amersham Corp. [5,6-^{3}H]UTP (40 Ci/mmol) and [8-^{3}H]GTP (15 Ci/mmol) were obtained from ICN Chemical and Radioisotope Division in a 50% ethanol solution. The ethanol was removed by lyophilization, and the nucleoside triphosphate was dissolved in the reaction medium. ATP, CTP, GTP, UTP, phosphoenolpyruvic acid, pyruvate kinase (type III), dextran sulfate 500, RNase A, and RNase T_1 were obtained from Sigma Chemical Co. DNase I was obtained from Worthington Diagnostics. Protein concentrations were determined with the Bio-Rad protein assay kit obtained from Bio-Rad Laboratories.

RESULTS

Absence of an RNA-dependent RNA polymerase in purified TGEV. To investigate the possibility that TGEV does possess a virion-associated, RNA-dependent RNA polymerase, we examined semipurified and purified viral preparations, using an RNA polymerase assay that was optimized for the Newcastle disease virus-associated enzyme (14). Table 1 shows that RNA polymerase activity in purified TGEV ranged from 0 to 0.0004 the levels measured in vesicular stomatitis virus. We conclude that there is no polymerase activity in the virion. The assay employed for the detection of cell-associated enzyme (see below) was also used, but was modified to include detergent, and no enzyme activity could be detected (data not shown).

TABLE 1. Absence of RNA polymerase in purified TGEV[a]

Expt	[^{3}H]UMP incorporation			
	Vesicular stomatitis virus[b]		TGEV	
	Counts[c]	Amt[d]	Counts[c]	Amt[d]
1[e]	32,082	62,100	10	8
2[f]	19,754	48,600	0	0
3[g]	19,598	49,100	28	20

[a] In each experiment virus was resuspended and assayed as described in the text.

[b] Vesicular stomatitis virus was purified as described in the text.

[c] Counts per minute per assay per hour.

[d] Femtomoles per milligram of protein per hour.

[e] Approximately 10^{10} PFU of TGEV were partially purified from 800 ml of tissue culture fluid and assayed directly. Tissue culture fluid harvested from cells at 24 h postinfection was clarified at 10,000 × *g* for 10 min, and virus was pelleted from the supernatant at 90,000 × *g* for 2 h through an 8-ml barrier of 20% (wt/wt) sucrose made up in TNE.

[f] Approximately 10^{10} PFU of TGEV were purified from 800 ml of supernatant fluids as described in the text, except that virus was first concentrated by sedimentation onto a 60% (wt/wt) sucrose cushion before resuspension and isopycnic sedimentation. Purified virus was pelleted and stored at −80°C for 1 week prior to assay.

[g] Approximately 10^{10} PFU of TGEV were purified from 800 ml of supernatant fluids as described in the text, except that virus was first concentrated by polyethylene glycol precipitation before resuspension and isopycnic sedimentation. For polyethylene glycol precipitation, clarified supernatant was made 10% final concentration with polyethylene glycol (6000)–0.1 M NaCl–0.001 M EDTA and chilled at 0°C for 0.5 h with constant stirring. The precipitate was pelleted at 1,500 × *g* for 40 min at 0°C. The pellet was resuspended by Dounce homogenization prior to isopycnic sedimentation.

Kinetics of viral RNA synthesis in vivo. To maximize the chances of detecting an intracellular, virus-specific, RNA-dependent RNA polymerase, we made a systematic effort first to define the time period in which viral RNA was synthesized at a maximal rate and second to define the intracellular location of this synthesis. Preliminary experiments established that cellular RNA synthesis was inhibited by over 95% within 1 h when an actinomycin D concentration of 0.1 μg/ml was used. Actinomycin D concentrations of 0.1 to 1.0 μg/ml were therefore used in experiments designed to measure the synthesis of virus-specified RNA. The interval within the growth cycle of the virus during which viral RNA synthesis occurs at a maximal rate was determined by pulse labeling infected cells with radiolabeled uridine after a 1-h pretreatment

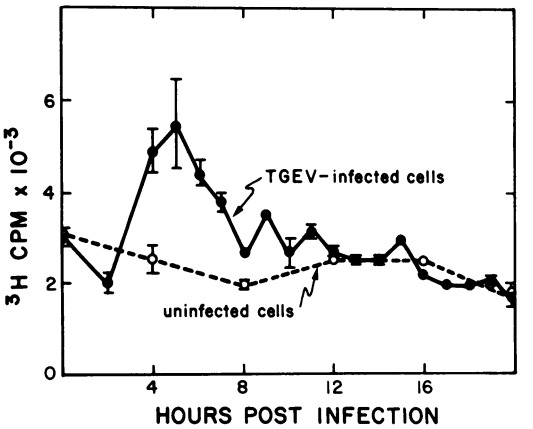

FIG. 1. Kinetics of viral RNA synthesis. Cells in 30-mm plates were infected simultaneously with TGEV at a multiplicity of 10 PFU per cell or mock infected with balanced salt solution and were refed with medium containing 2% fetal calf serum. At 1 h prior to labeling, actinomycin D was applied to the cells at a concentration of 0.1 μg/ml and kept there for the duration of the RNA labeling period. [^{3}H]uridine (4 μCi per plate) was added at various times postinfection for 1-h pulses. Periods were timed from the beginning of virus adsorption. Duplicate cultures were used for each time point. Cells were scraped into ice-cold 5% trichloroacetic acid–0.01 M sodium pyrophosphate, and the precipitate was collected on Whatman GF/F glass filters. Radioactivity was quantitated by scintillation spectrophotometry.

with actinomycin D (Fig. 1). The rate of RNA synthesis was found to be maximal (an average of 215,000 cpm per culture per h above synthesis in uninfected cells) between 4 and 6 h postinfection, with a peak rate of synthesis at around 5 h postinfection. Forty percent of the total RNA synthesized during the 19-h viral growth cycle (4) took place within this interval of time. Mock-infected cells showed no increase throughout the 20-h labeling period, indicating that the observed RNA synthesis is induced by the viral infection and probably represents virus-specific RNA synthesis.

Intracellular location of viral RNA synthesis. For the purpose of identifying a crude cellular fraction that possesses the TGEV RNA-synthesizing activity, we sought to isolate the fraction which contained TGEV-specified RNA at the end of a short pulse period. Essentially, an experimental protocol employed for the fractionation of picornavirus-infected cells was followed (7). Infected cells were pulse labeled between 5 and 5.5 h postinfection with [^{3}H]uridine and were immediately fractionated into the nuclear, mitochondrial, and postmitochondrial fractions. Each fraction was analyzed for acid-precipitable radioactivity (Table 2). The largest quantity of incorporated [^{3}H]uridine was found in the mitochondrial fraction of infected cells, which contained 80% of all the precipitable counts. This fraction also contained 50 times more counts than were found in the equivalent fraction from uninfected cells. A significant number of counts, representing 19% of the total, was found in the nuclear fraction of the infected cells, but this could be traced to contamination by membranous material of the type contained in the mitochondrial fraction. Successive washes of the nuclear fraction with 0.3 M sucrose followed by pelleting decreased the contamination as monitored by light microscopy, and there was a coincidental decrease in the amount of acid-precipitable radioactive material. We conclude, therefore, that the viral RNA-synthesizing structures were contained primarily in the mitochondrial fraction of infected cells.

Viral RNA polymerase activity in infected cells. Using a modification of an RNA polymerase assay that was optimized for the detection of the cell-associated, picornavirus RNA-dependent RNA polymerase (2), we sought an RNA polymerase activity in the cytoplasmic fraction of infected cells at 5 h postinfection (Table 3). More than 90% of the total cytoplasmic polymerase activity was associated with the mitochondrial fraction, and the activity found in this

TABLE 2. Intracellular location of viral RNA synthesis[a]

Fraction	[^{3}H]uridine incorporation (cpm)	
	Uninfected[b]	Infected
Nuclear	11,200 (43%[c])	165,700 (19%)
Mitochondrial	13,680 (53%)	693,960 (80%)
Postmitochondrial	880 (4%)	3,200 (1%)

[a] A roller culture of 2×10^8 cells was infected at a multiplicity of 10 PFU per cell, and an identical culture was mock infected with a balanced salt solution. Both cultures were fed with medium containing 2% fetal calf serum at the end of 1 h. At 3 h postinfection, timed from the beginning of the adsorption period, actinomycin D was added to make a final concentration of 1.0 μg/ml. At 5 h postinfection, this medium was replaced with 15 ml per bottle of medium containing 1.0 μg of actinomycin D per ml and 100 μCi of [^{3}H]uridine per ml. After 0.5 h of incubation at 37°C, cells were scraped from the bottles and fractionated as described in the text. Samples of each cellular fraction were assayed for acid-precipitable radioactive material.

[b] The amount of acid-precipitable, [^{3}H]uridine-labeled material in uninfected cells was less than 3% of that found in infected cells.

[c] Percentage of total. Percentages for each fraction were calculated as the percentage of the total incorporated into all three fractions.

TABLE 3. RNA polymerase activity in the cytoplasmic fraction of TGEV-infected cells[a]

Fraction	[3H]UMP incorporation					
	Uninfected			Infected		
	Counts[b]	Amt[c]	Total fmol/h (%)	Counts[b]	Amt[c]	Total fmol/h (%)
Nuclear	ND[d]			ND		
Mitochondrial	112	2.5	18 (45)	6,385	145	1,595 (96)
Postmitochondrial	136	3.1	22 (55)	289	6.5	60 (4)

[a] Separate roller cultures, each containing 2×10^8 cells, were infected at a multiplicity of 10 PFU per cell or mock infected with a balanced salt solution and were refed with medium containing 2% fetal calf serum. At 5 h postinfection, cells were scraped from the bottle and fractionated as described in the text. The mitochondrial and postmitochondrial fractions were assayed for RNA polymerase as described in the text.

[b] Counts per minute per assay per hour.

[c] Femtomoles per milligram of protein per hour.

[d] Not determined.

fraction was 10- to 100-fold greater than any similar activity detectable in the mitochondrial fraction from uninfected cells.

Characteristics of viral RNA polymerase activity. To examine the characteristics of the [3H]UMP incorporating activity, we sedimented cytoplasmic membranous structures containing the enzymatic activity through a barrier of 20% sucrose to prepare a postnuclear pellet (2). We then examined conditions for maximal activity and template requirements (Table 4). Polymerizing activity was reduced by 25% in the absence of Mg^{2+} and was reduced by 85% when Mn^{2+} was substituted for Mg^{2+}. The activity therefore apparently requires Mg^{2+}. No other divalent cations were tested. Polymerizing activity was reduced by only 2% in the absence of 2-mercaptoethanol, so a reducing agent is not required for full activity. No decrease in activity was observed when phosphoenolpyruvate and pyruvate kinase were omitted from the reaction mixture, suggesting that an ATP-generating system is not required. This may be evidence that ATPases which are normally present in crudely prepared mitochondrial fractions were removed by sedimentation through 20% sucrose (25). The presence of 20 μg of actinomycin D per ml in the reaction failed to inhibit [3H]UMP incorporation, and therefore the possibility that the product was made from a DNA template is precluded. Complete dependence on each of the supplementary ribonucleoside triphosphates for full activity was seen only when [3H]GTP was used for labeling. Greater than 50% inhibition of the polymerase activity resulted when each of the supplementary ribonucleoside triphosphates was omitted. Greater than 90% inhibition resulted when all three were omitted. This is most readily explained by a template dependence for the activity. When [3H]UTP was used for labeling, less than 20% inhibition was seen in the absence of CTP or GTP alone. It is therefore possible that we are measuring homoribopolymerase activity under these circumstances (8, 13). More than 90% of the activity was lost in the absence of all three supplementary nucleoside triphosphates, however, but this is probably a result of the dependence of the activity on added ATP. Since the enzyme was not inhibited by actinomycin D, we conclude that the template is RNA. The heat-denatured product was totally resistant to DNase but was 73% degraded by a mixture of pancreatic and T_1 RNases. We therefore conclude that the product is RNA.

Because of the reported beneficial effects of dextran sulfate as an RNase inhibitor in studies of RNA-polymerizing systems (1), it was included in our reaction mixture at a concentration of 40 μg/ml. To determine whether dextran sulfate has an inhibitory effect on the in vitro polymerase reaction, we measured the amount of product made in the absence of dextran sulfate. Removing dextran sulfate resulted in a 27% enhancement of activity. Increasing the dextran sulfate concentration 20-fold resulted in only a 4% inhibition of the reaction. Dextran sulfate was therefore routinely included in the reaction mixture for its possible protective effects on the reaction products when the reaction products were analyzed.

The optimal Mg^{2+} concentration for the polymerase reaction was approximately 5 mM (Fig. 2). Increasing concentrations above 5 mM caused an aggregation within the reaction mixture which had the appearance of a precipitate. This may have been the cause of the inhibition at the higher concentrations.

The kinetics of the [3H]UMP-incorporating activity at 37°C are shown in Fig. 3. The incorporation increased rapidly for the first 10 min and then decreased by more than 50% to remain constant for at least 50 min.

Preliminary evidence for a membrane-associated replication complex. Viral RNA synthesis in

TABLE 4. Characteristics of the RNA polymerase activity[a]

Sample	[^{3}H]UMP or [^{3}H]GMP incorporation (fmol/mg of protein per h)	% of complete reaction
Complete reaction[b]	137	100
Minus Mg^{2+}[b,c]	103	75
Minus Mg^{2+}, plus 2 mM Mn^{2+}[b,c]	20	15
Minus 2-mercaptoethanol[b]	134	98
Minus phosphoenolpyruvate (PEP) and PEP kinase[b]	142	104
Minus actinomycin D[b]	142	104
Minus ATP[b]	13	9
Minus CTP[b]	113	82
Minus GTP[b]	123	90
Minus ATP, CTP, and GTP[b]	3	2
Minus dextran sulfate[b]	175	127
Dextran sulfate[b] 200 μg/ml	129	94
Heated product plus DNase[b,d]	137	100
Heated product plus RNase[b,e]	37	27
Complete reaction[f]	286	100
Minus ATP[f]	123	43
Minus CTP[f]	29	10
Minus UTP[f]	87	31
Minus ATP, CTP, and UTP[f]	6	2

[a] For these reactions the assay was performed on a postnuclear fraction prepared in the following manner. Cells were harvested and lysed, and the nuclear fraction was prepared as described in the text. The supernatant from the nuclear pellet was brought to a 17-ml total volume by the addition of 0.3 M sucrose and layered onto a 20-ml cushion of 20% (wt/wt) sucrose–0.01 M Tris-hydrochloride (pH 7.4) in a 38-ml centrifuge tube. The pellet formed by centrifugation at 60,000 × *g* for 1.5 h at 4°C in a Sorvall AH-627 rotor was drained and suspended in a solution of 0.05 M Tris-hydrochloride (pH 8.0)–0.0015 M $MgCl_2$–2.8 mg of sodium deoxycholate per ml to a final protein concentration of 10 to 20 mg/ml as assayed by the Bio-Rad protein assay (Bio-Rad Laboratories).

[b] [^{3}H]UTP was used as the labeled nucleoside triphosphate.

[c] The postnuclear fraction for this reaction was resuspended in 0.05 M Tris-hydrochloride (pH 8.0)–2.8 mg of sodium deoxycholate per ml.

[d] At the end of the 60-min reaction, the entire reaction mixture was heated at 100°C for 2 min, cooled to 37°C, and treated with 50 μg of DNase I per ml for 15 min at 37°C. The reaction was then terminated, and the radioactivity was quantitated by scintillation spectrophotometry.

[e] At the end of the 60-min reaction, the entire reaction mixture was heated at 100°C for 2 min, cooled to 37°C, and treated with 20 μg of RNase A per ml and 20 U of T_1 RNase per ml for 15 min at 37°C. The reaction was then terminated, and the radioactivity was quantitated by scintillation spectrophotometry.

[f] [^{3}H]GTP was used as the labeled nucleoside triphosphate.

both picornavirus-infected cells (2, 5, 7, 9, 12) and togavirus-infected cells (6, 11, 24, 26) has been shown to take place in a ribonucleoprotein complex called the replication complex. The replication complex by definition consists of the template for viral RNA replication, replicating strands of viral RNA (replicative intermediate), and viral RNA polymerase (11, 12). In addition, the replication complex is membrane bound and is released from membranes by treatment with nonionic detergents (2, 5, 6, 11, 12, 25, 26, 33). Two pieces of preliminary evidence suggest that TGEV RNA is synthesized on a similar membrane-bound replication complex. First, the nonionic detergent deoxycholate reduced the sedimentation rate of pulse-labeled viral RNA and polymerase activity. Table 2 shows that 80% of virus-specific RNA labeled within a 0.5-h pulse period sedimented to a pellet at 13,000 × *g* for 20 min in 0.3 M sucrose. Table 3 shows that more than 90% of total cytoplasmic polymerase activity was also pelleted under these conditions. Both pulse-labeled viral RNA and viral polymerase activity therefore have sedimentation coefficients far greater than 500S when no detergent is employed in the fractionation procedure. When the postnuclear preparation was first treated with 1% deoxycholate and then sedimented in the presence of 1% deoxycholate, the sedimentation rate of both the virus-specific RNA and polymerase activity was measured to be much less than 500S (Fig. 4). Second, the polymerase and about one-half of the pulse-labeled RNA cosedimented in a rate-zonal gradient in the presence of detergent (Fig. 4). Relative to the sedimentation of 160S poliovirus (22), pulse-labeled viral RNA sedimented as a broad peak from the top of the gradient to about 200S,

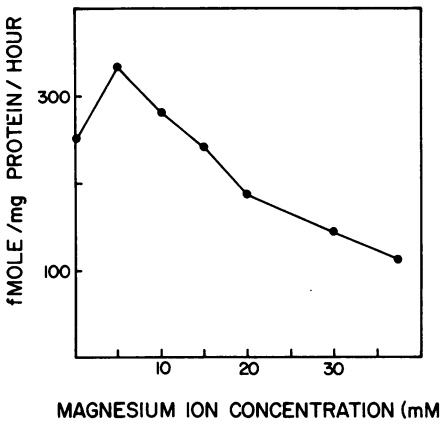

FIG. 2. RNA polymerase activity as a function of magnesium ion concentration. [^{3}H]UMP incorporation was measured as a function of Mg^{2+} concentration. The preparation of the postnuclear fraction and the reaction conditions were as described in Table 4, footnote *a*.

with a peak at around 108S (Fig. 4A). Viral polymerase activity sedimented as two peaks, one in the range of 45 to 140S and one in the range of 200 to 300S (Fig. 4B).

Whether the two peaks of RNA polymerase activity on the gradient described in Fig. 4B represent two different polymerases or two forms of the same polymerase has not been determined. The uninfected cell preparation demonstrated no polymerase activity in the upper half of the gradient but did exhibit some activity in the bottom two fractions of the gradient. This may represent a cellular RNA polymerase, perhaps of mitochondrial origin, that is insensitive to actinomycin D (25). It is perhaps this activity that we are detecting in the mitochondrial fractions of uninfected cells (Table 2).

Virus-specific RNA in infected cells. To confirm the viral specificity of the RNA-dependent RNA polymerase activity, we compared the products of the in vitro reaction with viral RNA species made in vivo. To examine the RNA species made at the time the rate of RNA synthesis is maximal, we labeled infected cells with [^{3}H]uridine in the presence of actinomycin D between 5 and 5.5 h postinfection. The RNA was extracted from the postnuclear pellet and examined under denaturing conditions by electrophoresis on agarose gels (Fig. 5 and 6). Six major species, on the basis of total incorporated radiolabeled uridine, with apparent molecular weights of 6.8×10^6, 6.2×10^6, 3.15×10^6, 1.40×10^6, 0.94×10^6, and 0.66×10^6, were resolved. Unresolved species were present in the lower quarter of the gel. The same species were observed when total cytoplasmic RNA, extracted by the method of Erikson et al. (10), was examined (data not shown). Molecular weights were estimated by extrapolation and interpolation from a plot of the molecular weight versus relative mobility for known single-stranded RNA markers which included vesicular stomatitis virus RNA (3.8×10^6 molecular weight [28]), 28S and 18S MDBK cell rRNA (1.75×10^6 and 0.68×10^6 molecular weight, respectively), and 23S and 16S *Escherichia coli* rRNA (1.1×10^6 and 0.56×10^6 molecular weight, respectively) (4 and data not shown). The 6.8×10^6-molecular-weight species comigrated with TGEV genomic RNA (data not shown). No RNA could be observed in extracts from uninfected cells, even though the total rate of RNA synthesis under identical conditions was 3% of that in infected cells (data not shown).

Polyadenylation of intracellular virus-specified RNA. To determine whether intracellular virus-specified RNA is polyadenylated, we pulse labeled infected cells with [^{3}H]uridine between 5 and 5.5 h postinfection in the presence of actinomycin D. RNA was extracted from the postnuclear pellet and chromatographed on oligodeoxythymidylate-cellulose. All six of the major RNA species described above were polyadenylated by this criterion. In addition, four minor polyadenylated RNA species with molecular weights of 1.05×10^6, 0.39×10^6, 0.34×10^6, and 0.24×10^6 were resolved (Fig. 5 and 6). Some of the 6.8×10^6-, 1.40×10^6-, and 0.66×10^6-molecular-weight species appeared to be non-polyadenylated (Fig. 5 and 6).

Single-stranded nature of intracellular virus-specified RNA. All RNA species extracted from

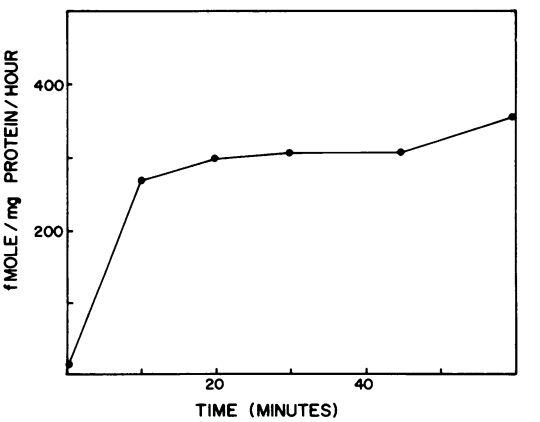

FIG. 3. Kinetics of the in vitro polymerase reaction. [^{3}H]UMP incorporation was measured as a function of time. The preparation of the postnuclear fraction and the reaction conditions were as described in Table 4, footnote *a*.

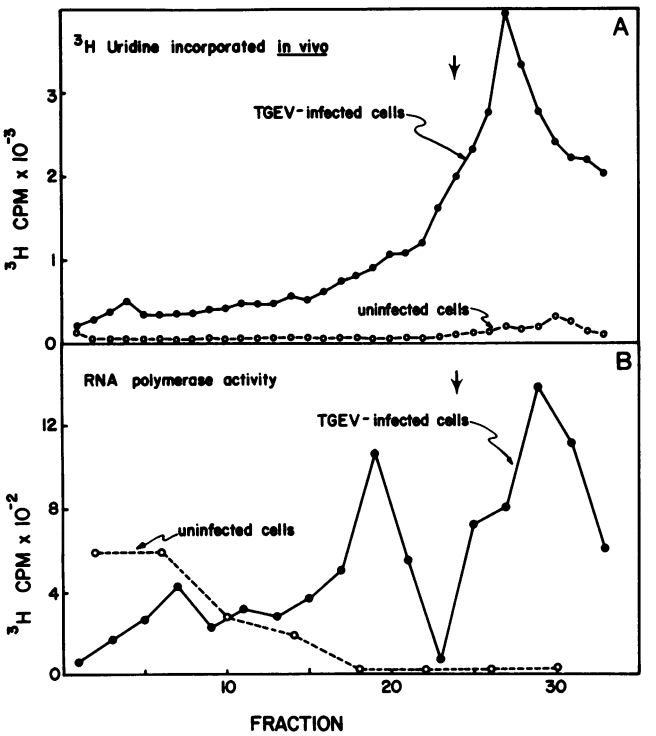

FIG. 4. Rate zonal sedimentation of deoxycholate-solubilized postnuclear fraction. (A) Cells in roller culture (2×10^8 cells) were infected at a multiplicity of 10 PFU/cell, and an identical culture was mock infected with a balanced salt solution. Both cultures were refed with medium containing 2% fetal calf serum at the end of a 1-h adsorption period. At 3 h postinfection, timed from the beginning of the adsorption period, actinomycin D was added to make a final concentration of 1.0 μg/ml. At 5 h postinfection, 1,000 μCi of [^{3}H]uridine was added per culture, and cells were incubated for 0.5 h at 37°C. Cells were then harvested and fractionated as described in the text, except that they were swollen and lysed by Dounce homogenization in 0.3 M sucrose–0.0015 M $MgCl_2$. The postnuclear supernatant was prepared as described in the text and immediately made 1% (wt/wt) final concentration with sodium deoxycholate. The preparation was then sedimented on a 15 to 40% (wt/wt) sucrose gradient which contained a 1% (wt/wt) final concentration of sodium deoxycholate. Sucrose solutions were made in 0.01 M Tris-hydrochloride (pH 7.4). Sedimentation was at 26,000 × *g* for 1.5 h at 4°C in a Beckman SW41 rotor, and the gradients were fractionated and analyzed for acid-precipitable radioactivity. (B) Infected and uninfected cells, 2×10^8 each, were treated and fractionated in parallel with those described in A, except that they were not isotopically labeled. Selected fractions of the gradient were assayed for [^{3}H]UMP-incorporating activity. The arrow indicates the position of 160S poliovirus sedimented under identical conditions. Sedimentation was from right to left.

infected cells were single stranded, as judged by their sensitivity to digestion with RNase T_1 in 0.3 M NaCl (Fig. 6). It is possible that double-stranded replicative intermediates were present but in numbers too few to be detected by this method.

Relative molar concentrations of the polyadenylated intracellular virus-specified RNA species. The percentage composition and relative molar concentrations of the intracellular polyadenylated RNA species were estimated by analyzing microdensitometer tracings of fluorograms. The results are given in Table 5.

Viral RNA species synthesized during the in vitro polymerase reaction. To examine the RNA products of the in vitro polymerase reaction and to compare these directly with viral RNA species made in vivo, we analyzed both by electrophoresis on the same agarose slab gel after denaturation (Fig. 5). By these analyses, three in vitro transcripts were observed. The largest transcript migrated more slowly than virion RNA and is referred to as the high-molecular-weight (hmw) RNA. The second and third transcripts comigrated with the in vivo-synthesized 1.40×10^6- and 0.66×10^6-molecular-weight species. In addition, a possible fourth species that comigrated with the in vivo-synthesized 3.15×10^6-molecular-weight species was sometimes observed (Fig. 5). All of the in vitro

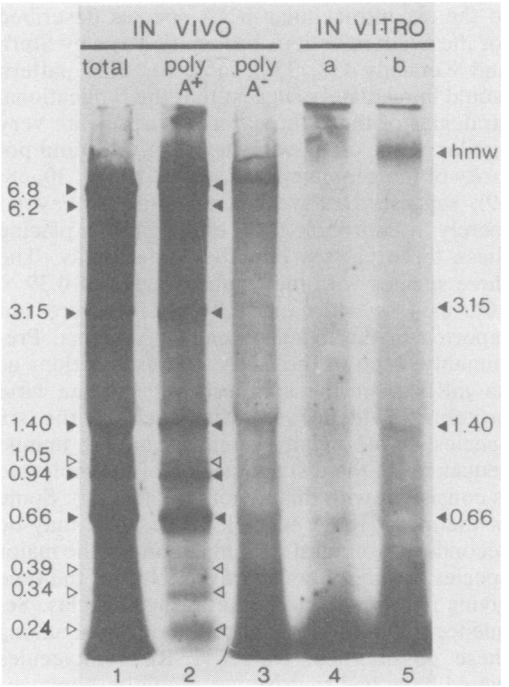

FIG. 5. Electrophoresis of virus-specified cytoplasmic RNA and in vitro polymerase products. Radiolabeled RNA extracted from the postnuclear pellet of infected cells prepared as described in the legend to Fig. 4 was electrophoresed after the indicated treatments. Lane 1, no treatment. Lanes 2 and 3, oligodeoxythymidylate-cellulose chromatography. In lanes 4 and 5, radiolabeled in vitro reaction products from two separate experiments (a and b) were extracted as described in the text and electrophoresed. The designation hmw represents high-molecular-weight RNA.

transcripts were susceptible to RNase T_1 digestion in high (0.3 M) NaCl (Fig. 6).

DISCUSSION

Our results indicate that the TGEV virion does not possess an RNA-dependent RNA polymerase but that the virus induces an enzyme of this type during replication. The absence of this enzyme on the virion, along with an infectious single-stranded RNA genome (4), are properties shared by both picornaviruses and togaviruses. Questions comparing the nature of the three virus systems are therefore raised. Basic requirements for the TGEV polymerase summarized in Table 4 are not unlike those described for picornaviruses (1, 2, 9, 13, 25) and alphatogaviruses (11, 24, 26, 33). A significant dependence of the enzyme on the presence of all three supplementary ribonucleoside triphosphates for full activity suggests that the majority of the activity is template dependent. Whether we are observing any homoribopolymer synthesis that might explain high [^{3}H]UMP incorporation in the absence of CTP or GTP (Table 4) is not known. Homoribopolymer synthesis has been observed with certain isolated picornavirus replication complexes (8). We did not observe enhanced [^{3}H]UMP incorporation in the absence of supplementary nucleoside triphosphates, however, which was a property of the picornavirus-associated polyuridylic acid polymerase activity (8).

We do not know what portion of the [^{3}H]uridine-labeled material in the mitochondrial pellet might be associated with polyribosomes since we did not dissociate polyribosomes with chelating agents prior to sedimentation. We would expect some polyribosomal association since our pulse-labeling period (0.5 h) was relatively long. Cosedimentation of greater than 50% of the in vivo-labeled RNA with approximately 50% of the polymerase activity after deoxycholate treatment suggests, however, that a majority of the in vivo-labeled RNA is complexed to a replicational structure.

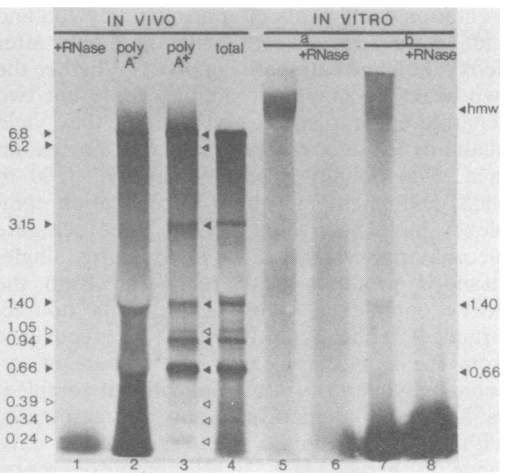

FIG. 6. RNase susceptibility of intracellular virus-specified RNA and in vitro polymerase products. Radiolabeled RNA from the postnuclear pellet of infected cells was prepared as described in the legend to Fig. 4 and was electrophoresed after the indicated treatments. Lane 1, digestion with 20 U of T_1 RNase per ml–0.3 M NaCl for 1 h at 37°C. Lanes 2 and 3, oligodeoxythymidylate-cellulose chromatography. Lane 4, no treatment. Radiolabeled in vitro reaction products from two separate experiments (a and b) were extracted as described in the text and electrophoresed after the indicated treatment. Lane 5, no treatment. Lane 6, RNase digestion as described for lane 1. Lane 7, no treatment. Lane 8, RNase digestion as described for lane 1. The designation hmw represents high-molecular-weight RNA.

TABLE 5. Percentage composition and relative molar concentration of polyadenylated viral RNA species synthesized in vivo[a]

RNA species (mol wt × 10^{-6})	Percentage composition[b]	Relative molar concn
6.8	28.3 ± 2.5	2.6
6.2	9.8 ± 1.7	1
3.15	8.5 ± 3.8	1.7
1.40	5.6 ± 1.0	2.5
1.05	3.1 ± 0.1	1.9
0.94	9.0 ± 0.6	6.1
0.66	27.2 ± 2.5	26.1
0.39	1.3 ± 0.2	2.1
0.34	2.2 ± 0.8	4.1
0.24	5.0 ± 2.8	13.2

[a] Radiolabeled, polyadenylated viral RNA was extracted from infected cells and analyzed by denaturing gel electrophoresis as described in the legend to Fig. 5.

[b] The percentage composition was determined from densitometric tracings of fluorograms from three separate experiments. Heterogeneous radioactive material within the gel was excluded from the quantitative analysis.

Two peaks of enzymatic activity with sedimentation coefficients of approximately 70S and 250S were seen in rate zonal gradients after deoxycholate treatment (Fig. 4B.). Whether the two peaks of enzymatic activity represent two separate enzyme species or whether they yield qualitatively different products was not examined. Functionally separate "heavy" (100 to 300S) and "light" (20 to 70S) replication complexes have been identified in three separate picornavirus systems (2, 5, 8). Primarily single-stranded products were recovered from the heavy complexes, whereas primarily double-stranded replicational forms were recovered from the light complexes. In the case of encephalomyocarditis virus replicational complexes, homoribopolymerase activity was associated with the light complex (8). Whether the existence of "heavy" and "light" complexes represents parallels in the replicational strategies of picornaviruses and coronaviruses is not known.

To confirm the viral specificity of the polymerase activity, we compared in vitro-synthesized products with viral RNA species made in vivo. Single-stranded, polyadenylated, actinomycin D-resistant RNA species with molecular weights of 6.8×10^6, 6.2×10^6, 3.15×10^6, 1.40×10^6, 1.05×10^6, 0.94×10^6, 0.66×10^6, 0.39×10^6, 0.34×10^6, and 0.24×10^6 were made in vivo. On first examination the seven largest of these would appear to correspond to the seven intracellular species described for the mouse hepatitis virus A59 by Spaan et al. (32), and six of the seven largest would appear to correspond to the six intracellular RNA species described for the avian infectious bronchitis virus by Stern and Kennedy (34, 35) (Table 6). This pattern would immediately suggest that the replicational strategies of these three coronaviruses are very similar. This, along with the positive-strand polarity of the genomic RNA (4, 16, 19, 20, 30, 38, 39), suggests that we can certainly go beyond merely a morphological criterion for placing these three viruses into the same family. The three species with molecular weights of 0.39×10^6, 0.34×10^6, and 0.24×10^6 were not reported in the avian or murine systems. Presumably, each of the RNA species functions as an mRNA for the synthesis of separate viral proteins. Evidence showing each of the six species in the avian system as having unique sequences in the distal 5′ region of the molecule is consistent with this hypothesis (34, 35). Some of the minor RNA species we describe may be secondary structural variants of one of the major species, or possibly defective RNAs of the type giving rise to defective interfering particles. Sequence data are required to differentiate among these possibilities. Defective RNA molecules would have had to arise very rapidly, however, since all of our experiments utilized virus stocks that were within 6 passages of plaque purification. Also present in infected cells were three species of RNA with molecular weights of 6.8×10^6, 1.40×10^6, and 0.66×10^6 which were not polyadenylated by our criterion. These may represent minus-strand species or, alternatively, positive-strand species on which polyadenylate tracts were missing or lost. Nucleotide sequence information is required to distinguish between these possibilities. The absence of RNase-resistant species suggests that double-stranded RNA forms are present in only very small numbers.

When the products of the in vitro polymerase reaction were examined by electrophoresis on denaturing gels, three species and possibly four were seen. The largest and most abundant species, representing up to 40% of the product, migrated more slowly than genomic RNA on denaturing agarose gels. Overdevelopment of gels revealed that a minor portion of the high-molecular-weight species was RNase resistant in 0.3 M salt, raising the possibility that it is a double-stranded replicative intermediate structure (data not shown). Such structures have been reported to be the major product of in vitro polymerase reactions in both picornavirus (150 and alphatogavirus (21) systems, and the same may also be true for this coronavirus system. The three smaller species have apparent molecular weights of 3.15×10^6, 1.40×10^6, and 0.66×10^6, and all appear to be single stranded.

It is not clear to us why only three of six major transcripts were obtained during the in vitro

TABLE 6. Size of coronavirus intracellular RNA species

Virus	RNA species (mol wt × 10^{-6})									
TGEV[a]	6.8,	6.2,	3.15,	1.40,	1.05,	0.94,	0.66,	0.39,	0.34,	0.24
Mouse hepatitis virus[b]	5.6,	4.0,	3.0,	1.4,	1.2,	0.9,	0.8,	—,	—,	—
Avian infections bronchitis virus[c]	5.9,	—,	2.6,	1.5,	1.3,	0.9,	0.6,	—,	—,	—

[a] From this study.
[b] From Spaan et al. (32).
[c] From Stern and Kennedy (34).

transcriptase reaction. Presumably, the in vitro reaction is serving to complete transcripts that have already been initiated. Preferential synthesis of three species suggests that a control mechanism is operating in vitro. We are not certain that these represent plus-stranded sequences. Preliminary data suggest that the two smaller in vitro transcripts, the 1.40×10^6- and 0.66×10^6-molecular-weight species, are not polyadenylated in vitro (data not shown). If in fact the transcripts represent positive, i.e., mRNA, strands, then polyadenylation must be an event that is separate from transcription. On the other hand, preliminary evidence suggests that the 3.14×10^6-molecular-weight species is polyadenylated in vitro (data not shown). For this species, polyadenylation is possibly a template-dependent transcriptional event, or it may be an event that is closely juxtaposed to transcription in time and space.

Studies are currently in progress to characterize TGEV structural and nonstructural proteins. Whether the cell-associated, RNA-dependent RNA polymerase is abundant enough to be detected by electrophoretic methods remains to be determined.

ACKNOWLEDGMENTS

This work was supported by Public Health Service grant R23 AI 14367 from the National Institute of Allergy and Infectious Diseases.

LITERATURE CITED

1. **Arlinghaus, R. B., and J. Polatnick.** 1967. Detergent-solubilized RNA polymerase from cells infected with foot-and-mouth disease virus. Science **158**:1320–1322.
2. **Arlinghaus, R. B., and J. Polatnick.** 1968. The isolation of two enzyme-ribonucleic acid complexes involved in the synthesis of foot-and-mouth disease ribonucleic acid. Proc. Natl. Acad. Sci. U.S.A. **62**:821–828.
3. **Baltimore, D.** 1971. Expression of animal virus genomes. Bacteriol. Rev. **35**:235–241.
4. **Brian, D. A., D. E. Dennis, and J. S. Guy.** 1980. Genome of porcine transmissible gastroenteritis virus. J. Virol. **34**:410–415.
5. **Caliguiri, L. A.** 1974. Analysis of RNA associated with the poliovirus RNA replication complexes. Virology **58**:526–535.
6. **Clewley, J. P., and S. I. T. Kennedy.** 1976. Purification and polypeptide composition of Semliki Forest Virus RNA polymerase. J. Gen. Virol. **32**:395–411.
7. **Dalgarno, L., and E. M. Martin.** 1965. Studies on EMC viral RNA synthesis and its location in infected Krebs ascites cells. Virology **26**:450–465.
8. **Dalgarno, L., E. M. Martin, S. L. Liu, and T. S. Work.** 1966. Characterization of the products formed by the RNA polymerases of cells infected with encephalomyocarditis virus. J. Mol. Biol. **15**:77–91.
9. **Ehrenfeld, E., J. V. Maizel, and D. F. Summers.** 1970. Soluble RNA polymerase complex from poliovirus-infected HeLa cells. Virology **40**:840–846.
10. **Erikson, E., R. L. Erikson, B. Henry, and N. R. Pace.** 1973. Comparison of oligonucleotides produced by RNase T_1 digestion of 7S RNA from avian and murine oncornaviruses and from uninfected cells. Virology **53**:40–46.
11. **Friedman, R. M., J. G. Levin, P. M. Grimley, and I. K. Berezesky.** 1972. Membrane-associated replication complex in arbovirus infection. J. Virol. **10**:504–515.
12. **Girard, M., D. Baltimore, and J. E. Darnell.** 1967. The poliovirus replication complex: site for synthesis of poliovirus RNA. J. Mol. Biol. **24**:59–74.
13. **Horton, E., S.-L. Liu, E. M. Martin, and T. S. Work.** 1966. Properties of a virus-induced RNA polymerase in ascites cells infected with encephalomyocarditis virus. J. Mol. Biol. **15**:62–76.
14. **Huang, A. S., D. A. Baltimore, and M. A. Bratt.** 1971. Ribonucleic acid polymerase in virions of Newcastle disease virus: comparison with the vesicular stomatitis virus polymerase. J. Virol. **7**:389–394.
15. **Kolias, S. I., and N. J. Dimmock.** 1974. Rhinovirus RNA polymerase: products and kinetics of appearance in human diploid cells. J. Virol. **14**:1035–1039.
16. **Lai, M. M. C., and S. A. Stohlman.** 1978. RNA of mouse hepatitis virus. J. Virol. **26**:236–242.
17. **Laskey, R. A., and A. D. Mills.** 1975. Quantitative film detection of ^3H and ^{14}C in polyacrylamide gels by fluorography. Eur. J. Biochem. **56**:335–341.
18. **Lehrach, H., D. Diamond, J. Wozney, and H. Boedtker.** 1977. RNA molecular weight determinations by gel electrophoresis under denaturing conditions, a critical review. Biochemistry **16**:4743–4751.
19. **Lomniczi, B.** 1977. Biological properties of avian coronavirus RNA. J. Gen. Virol. **36**:531–533.
20. **Lomniczi, B., and I. Kennedy.** 1977. Genome of infectious bronchitis virus. J. Virol. **24**:99–107.
21. **Martin, E. M., and J. A. Sonnabend.** 1967. Ribonucleic acid polymerase catalyzing synthesis of double-stranded arbovirus ribonucleic acid. J. Virol. **1**:97–109.
22. **Martin, R. G., and B. N. Ames.** 1961. A method for determining the sedimentation behavior of enzymes: application to protein mixtures. J. Biol. Chem. **236**:1372–1379.
23. **McClurkin, A. W., and J. O. Norman.** 1966. Studies on transmissible gastroenteritis of swine. II. Selected characteristics of a cytopathogenic virus common to five isolates from transmissible gastroenteritis. Can. J. Comp. Med. Vet. Sci. **30**:190–198.
24. **Michel, M. R., and P. J. Gomatos.** 1973. Semliki forest virus-specific RNAs synthesized in vitro by enzyme from infected BHK cells. J. Virol. **11**:900–914.

25. **Plagemann, P. G. W., and H. E. Swim.** 1966. Symposium on replication of viral nucleic acids. III. Replication of mengovirus ribonucleic acid. Bacteriol. Rev. **30**:288–308.
26. **Qureshi, A. A., and D. W. Trent.** 1972. Saint Louis encephalitis virus ribonucleic acid replication complex. J. Virol. **9**:565–573.
27. **Rekosh, D. M. K.** 1977. The molecular biology of picornaviruses, p. 63–110. *In* D. P. Nayak (ed.), The molecular biology of animal viruses. Marcel Dekker, Inc., New York.
28. **Repik, P., and D. H. L. Bishop.** 1973. Determination of the molecular weight of animal RNA viral genomes by nuclease digestions. I. Vesicular stomatitis virus and its defective T particle. J. Virol. **12**:969–983.
29. **Rottier, P. J. M., W. J. M. Spaan, M. C. Horzinek, and B. A. M. van der Zeijst.** 1981. Translation of three mouse hepatitis virus strain A59 subgenomic RNAs in *Xenopus levis* oocytes. J. Virol. **38**:20–26.
30. **Schochetman, G., R. H. Stevens, and R. W. Simpson.** 1977. Presence of infectious polyadenylated RNA in the coronavirus avian bronchitis virus. Virology **77**:772–782.
31. **Siddell, S. G., H. Wege, A. Barthel, and V. ter Meulen.** 1980. Coronavirus JHM: cell-free synthesis of structural protein p60. J. Virol. **33**:10–17.
32. **Spaan, W. J. M., P. J. Rottier, M. C. Horzinek, and B. A. M. van der Zeijst.** 1981. Isolation and identification of virus-specific mRNA's in cells infected with mouse hepatitis virus (MHV-A59). Virology **108**:424–434.
33. **Sreevalsan, T., and F. H. Yin.** 1969. Sindbis virus-induced viral ribonucleic acid polymerase. J. Virol. **3**:599–604.
34. **Stern, D. F., and S. I. T. Kennedy,** 1980. Coronavirus multiplication strategy. I. Identification and characterization of virus-specified RNA. J. Virol. **34**:665–674.
35. **Stern, D. F., and S. I. T. Kennedy.** 1981. Coronavirus multiplication strategy. II. Mapping the avian infectious bronchitis intracellular RNA species to the genome. J. Virol. **36**:440–449.
36. **Strauss, J. H., and E. G. Strauss.** 1977. Togaviruses, p. 111–166. *In* D. P. Nayak (ed.), The molecular biology of animal viruses. Marcel Dekker, Inc., New York.
37. **Tyrrell, D. A. J., J. D. Almeida, C. H. Cunningham, W. R. Dowdle, M. S. Hofstad, K. McIntosh, M. Tajima, L. Y. Zakstelskaya, B. C. Easterday, A. Kapikian, and R. W. Bingham.** 1975. Coronaviridae. Intervirology **5**:76–82.
38. **Wege, H. A., A. Muller, and V. ter Meulen.** 1978. Genomic RNA of the murine coronavirus JHM. J. Gen. Virol. **41**:217–227.
39. **Yogo, Y., N. Hirano, S. Shibuta, and M. Matumoto.** 1977. Polyadenylate in the virion RNA of mouse hepatitis virus. J. Biochem. **82**:1103–1108.